Available on CMS information server

CMS NOTE 2006/015

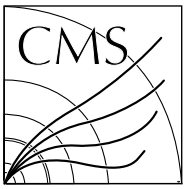

The Compact Muon Solenoid Experiment

CMS Note

Mailing address: CMS CERN, CH-1211 GENEVA 23, Switzerland

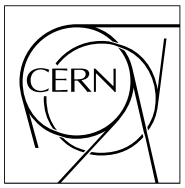

19 December 2005

Validation of the Simulation for the CMS Endcap Muon Cathode Strip Chamber Front-end Electronics

S. Durkin,

Department of Physics, Ohio State University, Columbus, OH 43210, USA

T. Ferguson[a)], N. Terentiev

Department of Physics, Carnegie Mellon University, Pittsburgh, PA 15213, USA

Abstract

The results of a validation of the ORCA simulation for the CMS Endcap Muon cathode strip chamber front-end electronics are presented. A comparison of the simulation results with test-beam and pulser calibration data is done for the cathode strip pulse shape and the cross-talk. The three types of data are compared using two methods – fitting the pulse shapes to find the shaping times and cross-talk coefficients, and directly comparing the pulse shapes and cross-talk time dependence. The ORCA description of the pulse shape is found to be adequate, though the cross-talk modeling could be updated using recent pulser calibration data as a basis.

[a)] Contact author: Thomas.Ferguson@cern.ch

1 Introduction

The CMS Endcap Muon cathode strip chambers (CSCs) provide the high coordinate precision and fast response time needed for good muon tracking and effective bunch-crossing number identification. The CSCs [1] are six-layer, two-coordinate-measuring, multiwire proportional chambers. In the geometry of CMS, the anode wires in each CSC layer run in the azimuthal direction and the cathode strips in the radial direction.

A realistic Monte Carlo simulation of the CSC input signals and electronics response was written [2], based on parameters available at the time of the preproduction electronics and the first test-beam results. In this simulation, particles are tracked through a CSC gas layer, generating a line of ionization electrons. Each electron is then transported to the nearest anode wire with a corresponding drift time and produces an avalanche charge. Half that amount of charge is induced on the cathode plane. This charge is distributed on the five nearest strips. Each drift electron produces a delta-function charge input on the strip. To create the analog signal seen by the cathode strip electronics, a parameterization of the amplifier and shaper response is convoluted with the ion drift collection time. The resulting signals from all the drift electron are then summed to form an output signal on the strip. Details of the simulation are available in [2].

A validation of this simulation, as it is performed in the ORCA software package [3], is important in view of the now-known parameter values of the final cathode-amplifier electronics and new experimental data from recent test-beam running in 2004 and special pulser calibration runs taken in 2005. The study described in this note was performed as part of the preparation for the CMS Physics TDR, Volume 1.

The test-beam layout included 5 CSCs of 4 different types (ME3/2, ME2/2, ME1/2, and 2 ME1/1) located in the CERN H2 beamline. The chambers were positioned to have a beam incident angle of 26° relative to normal incidence. Most of the data were taken with a 150 GeV/c muon beam, having an LHC-like 25 ns time structure. A self-triggering mode was employed, using the Endcap Muon Track-Finder electronics [4]. The main goal of the measurements was to test the production versions of the peripheral crate electronics, including the DAQ Motherboard (DMB) and Track-Finder modules. For the test-beam data analysis, only events with exactly one anode wire hit and one cathode comparator hit per CSC layer were selected so that there would be no confusion from multiple tracks.

The simulation data were obtained with the use of the OSCAR_3_7_0 [5] and ORCA_8_7_1 [3] packages in the full CMS detector geometry. Single-muon tracks with a p_T of 100 GeV/c were generated with flat distributions in η and ϕ. In the simulation data analysis, we require data from muon stations 2 and 3, and a reconstructed muon with $1.3 < \eta < 1.6$, in order to provide approximately the same average incident angle as in the test beam.

2 Description of the Pulse Shape Fitting Procedure

The output pulse from each cathode strip front-end amplifier channel is sampled every 50 ns and stored in a switched capacitor array (SCA) [6]. Eight consecutive SCA samples are digitized by a 12-bit, 40 MHz ADC and read out whenever a LCT · L1A coincidence is found (where LCT is a local charged track trigger and L1A is a Level-1 accept signal). The first 50 ns long SCA time bin is defined to be in coincidence with the L1A signal.

The SCA values, $SCA(t)$, in the time bins near the pulse height maximum are fit as a function of time by a 5-pole semi-Gaussian function $S(t)$, where $SCA(t) = Q \cdot S(t)$ and $S(t)$ is of the form:

$$S(t) = (0.2133)\left[\frac{t - T_s}{T_0}\right]^4 e^{-(t-T_s)/T_0}, \quad (1)$$

with $t - T_s > 0$. Here, Q is the total charge on the strip, T_s is the pulse arrival time, T_0 is $\frac{1}{4}$ of the pulse peaking time (see Figure 1), and the normalization constant is chosen so that $S(t) = 1$ at $t - T_s = 4 \cdot T_0$. Due to the 25 ns beam structure and the 50 ns SCA sampling period, a signal can have two possible positions in time (two T_s values), corresponding to whether the muon comes on an odd- or even-numbered L1A. Figure 1 shows an example of two pulses 25 ns apart and having their maximum SCA value in the same time bin at $t = 250$ ns. The particular T_s value also depends on the clock delay setting of the individual DMB, which can vary from board to board. In addition, the T_s value is smeared by the electron drift time in the chamber gas gap.

The fitting procedure uses $SCA(t)$ measurements from three adjacent cathode strips, with the middle strip having the maximum $SCA(t)$ value. Instead of taking 3 time bins centered on the one with the maximum charge deposition, as was done in a previous analysis, here 4 time bins are used, making a total of 12 measurements to fit.

Table 1 shows an example of the baseline-subtracted $SCA(t)$ values for 8 time bins and 3 cathode strips from one event. Adding one more bin at a earlier time ($t = 125$ ns) significantly reduces the correlation between the errors on T_s and T_0 from the fit.

Table 1: Baseline-subtracted SCA values for 8 time bins and 3 cathode strips from one event. The 12 values between the 2 vertical lines are used in the fit.

Strip\t (ns)	**25**	**75**	**125**	**175**	**225**	**275**	**325**	**375**
Left	0	0	41	110	88	41	18	5
Middle	0	3	112	420	512	370	214	122
Right	0	1	33	85	57	16	6	3

Measurements in the time bins at $t = 125, 175, 225$, and 275 ns are used in the fit, with the maximum SCA value for the middle strip being in the $t = 225$ ns time bin. The SCA value in the first time bin for each strip is used as the baseline for all the other time bins of that strip. An r.m.s. value of 2.7 counts for the baseline was found in the test-beam run, while the ORCA simulation uses an older r.m.s. estimate of 4.0 counts.

The function for fitting the ADC counts in 12 SCA time bins from 3 cathode strips in a given CSC layer uses the following simplified form:

$$SCA_{left}(t) \; = \; Q_{left} \cdot S(t) \; + \; Q_{middle} \cdot C_t \cdot F_c(t), \tag{2}$$

$$SCA_{middle}(t) = Q_{middle} \cdot S(t) \; + \; (Q_{left} + Q_{right}) \cdot C_t \cdot F_c(t), \tag{3}$$

$$SCA_{right}(t) \; = \; Q_{right} \cdot S(t) \; + \; Q_{middle} \cdot C_t \cdot F_c(t), \tag{4}$$

where Q_{left}, Q_{middle}, and Q_{right} are the total charges on the 3 strips, $S(t)$ is given by Equation (1), C_t is the cross-talk coefficient, and $F_c(t)$ is the cross-talk function describing the shape of the strip-to-strip cross-talk as a function of time (see the next section for more discussion).

For both the test-beam and simulation data, the fitted parameters are Q_{left}, Q_{middle}, Q_{right}, T_0, T_s, and C_t, giving a total number degrees of freedom in the fit of 6. The fit is done using the MINUIT package in the ROOT environment [7]. For a good measurement of the cross-talk coefficient, C_t, additional cuts are imposed on the cathode hits in the test-beam and simulation events. Only hits with a large pulse height and with the associated muon track coming close to the center of the middle strip are selected, yielding a selection efficiency of $\approx 10\%$.

3 Analysis Results

3.1 Measurement of the cross-talk from pulser data

Before giving the results of the fit described above, we discuss an independent determination of the cross-talk parameters, including the shape of the cross-talk pulse on the neighboring strips, using data taken in 2005 on a ME2/2 CSC at SX5 with an external pulser. The shape of the observed signal on the pulsed strip is basically the amplifier's response to a delta function charge input. To use this in the determination of the cross-talk for a real muon signal pulse, the pulser data are convoluted with an ion drift-time distribution and a flat time distribution for the cascading electrons. The resulting signal shape is fit to the semi-Gaussian function given in Equation (1). The cross-talk time dependence on the 2 adjacent strips is described by the function $F_c(t)$:

$$F_c(t) \; = \; buckeye\_pulse\_full(t, P_0, P_1, Z_1)/N, \tag{5}$$

where $buckeye\_pulse\_full(t, P_0, P_1, Z_1)$ is a specialized function, and N normalizes $F_c(t)$ to 1.0 at the pulse maximum for a given set of P_0, P_1 and Z_1 values. This parameterization of $F_c(t)$ describes the response of a resistance-capacitance circuit to a driving function $S(t)$.

Note that the current ORCA simulation [2] models the cross-talk with two components as well, one capacitive and one resistive. However, the ORCA simulation approximates it by making the capacitive component proportional to the slope of the signal, and the resistive component ($\approx 2\%$) proportional to the signal itself.

The convoluted pulser data from the pulsed middle strip and the 2 side strips with the cross-talk are fit using the following functions:

$$SCA_{left}(t) \;=\; Q \cdot C_t \cdot F_c(t), \tag{6}$$

$$SCA_{middle}(t) \;=\; Q \cdot S(t), \tag{7}$$

$$SCA_{right}(t) \;=\; Q \cdot C_t \cdot F_c(t), \tag{8}$$

where Q is the charge on the pulsed (middle) strip, which is normalized to have a maximum of 1.0.

The fitted parameters include the following:

Q – the charge on the pulsed (middle) strip,

T_0 – $\frac{1}{4}$ of the pulse peaking time,

T_s – the signal pulse arrival time,

C_t – the cross-talk coefficient,

T_{0c}, P_1, and Z_1 – parameters in the function $F_c(t) = buckeye\_pulse\_full(t, P_0, P_1, Z_1)$, with $P_0 = 1/T_{0c}$,

T_{sc} – the cross-talk pulse arrival time.

We subtract off the cross-talk pulse arrival time, $t \rightarrow t - T_{sc}$, for inputting values of the time to the function $buckeye\_pulse\_full(t, P_0, P_1, Z_1)$. The fit of the pulser data with T_{sc} equal to T_s does not significantly change the values of the other parameters. Therefore, in the fits to the test-beam and simulation data, the pulse arrival time for the cross-talk and signal pulses are set equal, $T_{sc} = T_s$.

There are a total of 8 fitted parameters for 119 points of pulser data, taken in steps of 6.25 ns. The fit is done using the ROOT program, with an arbitrary error of 0.01 used in the input to the $buckeye\_pulse\_full(t, P_0, P_1, Z_1)$ function. The results of the fit are shown in Figure 2. The residuals from the fit are all less than 0.035 for the signal pulse shape fit and less than 0.01 for the cross-talk fit on the side strips. The cross-talk coefficient, C_t, is found to be ≈ 0.1. The value of the Q parameter from the fit ($Q \approx 0.98$) is probably slightly biased due to the use of the semi-Gaussian function, $S(t)$, which does not model perfectly the tail of the pulse shape. The parameters $P_0 = 1/T_{0c} = 0.0334$ ns^{-1}, $P_1 = 0.03392$, $Z_1 = 0.00512$, and the corresponding value for $N = 0.458$ found from the fit are then fixed to these values in the following analysis of the test-beam and simulation data.

The stability of the fitted parameters T_0, Q, and C_t is studied by using the same pulser data, but shifting the 50 ns time window 8 times in steps of 6.25 ns, in such a way that the maximum of the central peak remains within the same time bin. The parameters P_0, P_1, Z_1, and N in the cross-talk function $F_c(t)$ are held fixed. As for the test-beam and simulation data analysis, 4 time bins are used in the fit. The values of the parameters Q, T_s, T_0, and C_t versus the time window step position are shown in Figure 3. As expected, the dependence of the pulse arrival time, T_s, on the peak position time is approximately linear with a slope close to 1.0 (≈ 0.96), while Q, T_0, and C_t remain almost constant (Q = 0.98 − 0.99, T_0 = 34.1 − 36.0 ns, and C_t = 0.095 − 0.098).

3.2 Results of the pulse shape parameter fits

We now present the results of fitting the pulse shapes from the test-beam and simulation data, described in Section 2, and compare them to the values found from fitting the pulser data, discussed in the previous section. The fitted values of the peaking time, T_0, from the pulser data (34-36 ns) and the ORCA simulation (34 ns) (Figure 4) are quite consistent, and are also very similar to the values from the test-beam data for the ME1/2, ME2/2 and ME3/2 chambers (the distribution for the ME2/2 chamber is shown in Figure 5). The average peaking time is slightly smaller for the 2 ME1/1 chambers (Figure 6) that have a smaller gas gap.

The measured cross-talk coefficient, C_t, is quite similar (≈ 0.1) for the pulser and test-beam data among chambers with the same strip geometry, ME2/2 and ME3/2 (the ME2/2 distribution is shown in Figure 7), but is less for the ME1/2 chamber (Figure 8) that has a strip geometry and capacitance different from the ME23/2 chambers. The mean of the C_t distribution from the ORCA simulation (≈ 0.08, Figure 9) is lower than in the test-beam and pulser data, likely due to the simplified cross-talk description used in ORCA.

The above comparison of the 3 types of data is done with the fitted parameters of the pulse shape and cross-talk. However, using the SCA data itself and one of the fitted parameters, the pulse arrival time T_s, we can directly compare the cathode strip pulse shape and the cross-talk in the test-beam, simulation, and pulser data (see subsections 3.4 and 3.5 below). This comparison is the main focus of the note.

The arrival time of the cathode strip pulse can also be used in an offline data analysis to measure with high precision the muon beam-crossing time. We show how this can be done in the next subsection.

3.3 Measurement of the muon beam-crossing time

The distribution of the measured pulse arrival times, T_s, for one ME3/2 CSC layer (Figure 10) in the test-beam data shows two peaks, 25 ns apart, which are smeared due to the electron drift time in that layer. The two peaks are due to the coupling of the 25 ns beam structure and the 50 ns SCA sampling time, as was discussed previously. Averaging the measured arrival times from the 6 layers of a CSC on an event-by-event basis substantially reduces this smearing and gives a measurement of the muon beam-crossing time with high precision. The corresponding muon beam-crossing time distributions are given for the ME1/2 (Figure 11), ME2/2 (Figure 12), and ME3/2 (Figure 13) CSCs. The variation in the widths of the peaks is due to the different positions of the first SCA time bin used in the fit. When pulse shapes are sampled and fitted with a limited number of points, the fit is sensitive to the positions of the points. For example, when the first SCA time bin samples the very beginning of the pulse (its rising edge), this time bin contributes less to the overall fit, making the measurement of T_s less precise.

3.4 Restoring the pulse shape

The dependence of $SCA(t)$ on T_s can be eliminated by subtracting the fitted T_s value from the times of all 8 SCA samples for a given cathode strip in each event. We call the result the "restored" pulse shape. Since T_s has a distribution of values, the SCA samples each pulse at different times. By subtracting off T_s and averaging over many pulses, the restored pulse shape will be measured at many more time points than the original 8 time bins. Figure 14 shows the resulting pulse shape distribution for pulses on the middle strip of an ME3/2 CSC from test-beam data. Averaging the quantity $SCA(t - T_s)/Q$ for each 6.25 ns time bin gives the restored pulse shape. Figure 15 compares this shape with those from the ME1/2 and ME2/2 CSCs. All 3 chamber types give very similar pulse shapes. A similar procedure is done using both the ORCA simulated data and the pulser data. A comparison of the resulting pulse shapes with the ME2/2 test-beam one (Figure 16) shows excellent agreement.

Note that the ORCA simulation uses an older cathode amplifier single-electron response function [8]. A more up-to-date function, based on the measured parameters of the final cathode-amplifier electronics, is compared to the old one in Figure 17. The difference between the 2 functions is rather small, which explains why the pulse shape from the ORCA simulation is in good agreement with those from the test-beam and pulser data.

3.5 Measuring the cross-talk with the restored pulse shape

In a previous analysis of the pulser data, the cross-talk versus time relationship was measured as the ratio of the SCA value for one side strip to the sum of the central strip and both side strip SCAs for a given time bin. We present here measurements obtained in a similar manner of the cross-talk distributions for the test-beam, pulser, and simulation data, using the T_s subtraction method to restore the pulse shapes. Again, hits with a large signal and from muons close to the center of the middle strip are selected to provide a reliable cross-talk measurement. For a direct comparison with the pulser data, where only the central strip was pulsed, the contribution of the induced charge from the track hit on the side strip SCAs is eliminated by subtracting the fitted values of $Q_{left} \cdot S(t)$ and $Q_{right} \cdot S(t)$ from the corresponding SCA in the 4 time bins. The corresponding cross-talk-averaged ratios are presented in Figure 18. They show reasonable agreement between the cross-talk from the test-beam and pulser data. The cross-talk in the ORCA simulation is clearly different from the measurements in both the test-beam and pulser data. This is attributable to the ORCA modeling in which the cross-talk is taken as a simple derivative of the central peak, while the real cross-talk dependence is now understood to be more complex.

In this note, we have ignored the effect of charge conservation where the pulse on the middle strip is diminished by the cross-talk charge transferred to the two adjacent strips. This effect is small, corresponding to a small shift in the parameter T_0 ($\approx$3 ns) on the center-strip pulse for all three types of data. Since all the data are treated identically, our empirical results remain valid.

4 Summary

Three types of data, from test beam, pulser, and ORCA simulation, have been compared by using two different methods: (a) fitting their respective pulse shapes and comparing the fitted parameters of peaking time and cross-talk, and (b) doing a direct comparison of their restored pulse shapes and cross-talk time dependencies.

From these comparisons, we find that the shape of the cathode strip output pulses in the ORCA simulation and in the test-beam and pulser data are quite similar. This agrees with the rather small difference in the old and new cathode amplifier single-electron response functions. For consistency, though, the new single-electron response function should replace the old one in the ORCA simulation.

The measurements of the cross-talk parameter in the test-beam and pulser data are consistent. The cross-talk in the ORCA simulation, however, differs from the other two at the level of about 15%, and the simulation should be updated by incorporating the corresponding function.

5 Acknowledgments

We are grateful to Timothy Cox, Richard Wilkinson, Eric James, Martijn Mulders, Richard Breedon, and Darin Acosta for very useful discussions and encouragement.

References

[1] D. Acosta et al., *Large CMS Cathode Strip Chambers: Design and Performance*, Nucl. Instr. and Meth. **A 453** (2000) 182.

[2] R. Wilkinson and P.T. Cox, *Simulating the Endcap Muon CSC system in ORCA*, CMS Note 2001/013.

[3] *CMS OO Reconstruction*, http://cmsdoc.cern.ch/orca/.

[4] D. Acosta et al., *Performance of a Pre-Production Track-Finding Processor for the Level-1 Trigger of the CMS Endcap Muon System*, Proceedings of the 10th Workshop on electronics for LHC experiments, Boston, Massachusetts, 13-17 September, 2004.

[5] *Object-Oriented Simulation for CMS Analysis and Reconstruction (OSCAR)*, http://cmsdoc.cern.ch/oscar/.

[6] R.E. Breedon et al., *Performance and Radiation Testing of a Low-Noise Switched Capacitor Array for the CMS Endcap Muon System*, Proceedings of the Sixth Workshop on Electronics for LHC Experiments, Krakow, Poland, CERN/LHCC/2000-041 (2000) 187-191.

[7] *ROOT: An Object-Oriented Data Analysis Framework*, http://root.cern.ch/.

[8] R. Wilkinson, private communication.

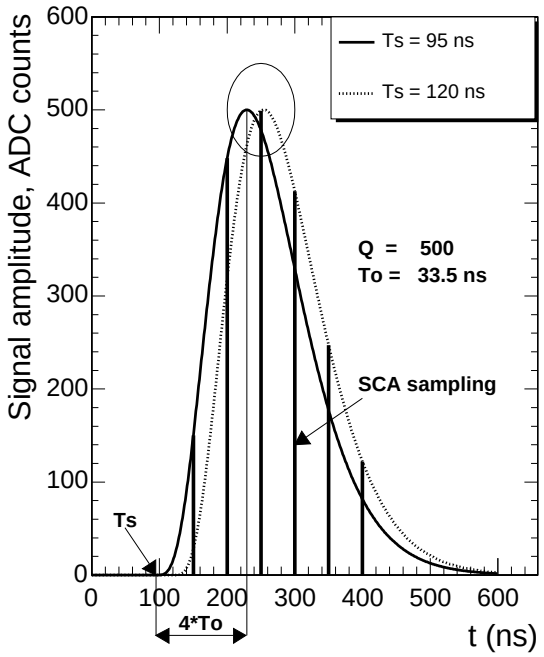

Figure 1: Example of 2 cathode strip pulses with the same peaking time ($4T_0$), but with different arrival times (T_s). The SCA sampling times are shown by the vertical lines.

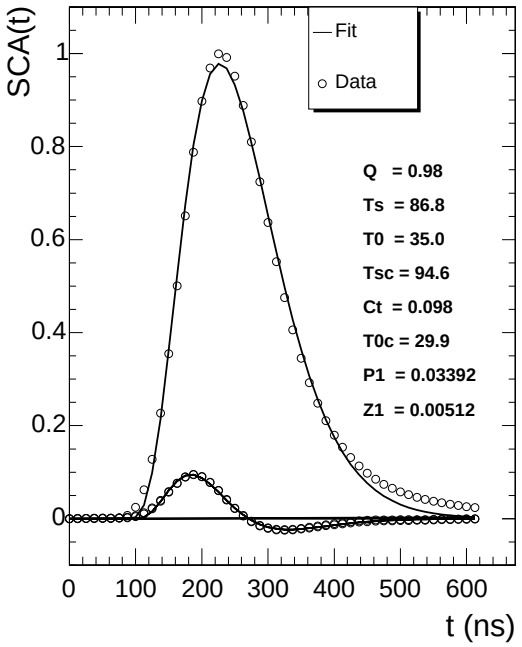

Figure 2: Results of the fit for the middle-strip pulse shape (larger pulse) and for the 2 side-strip cross-talk pulse shapes (smaller pulse) from the pulser data.

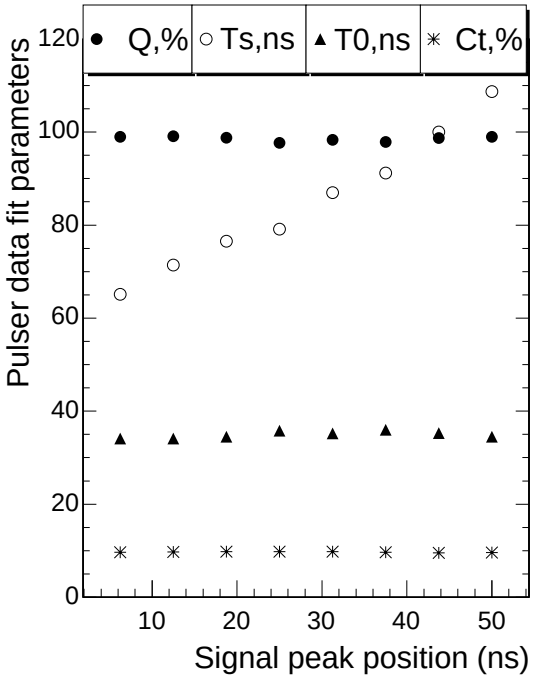

Figure 3: Dependence of the fitted pulse shape parameters on the signal peak position.

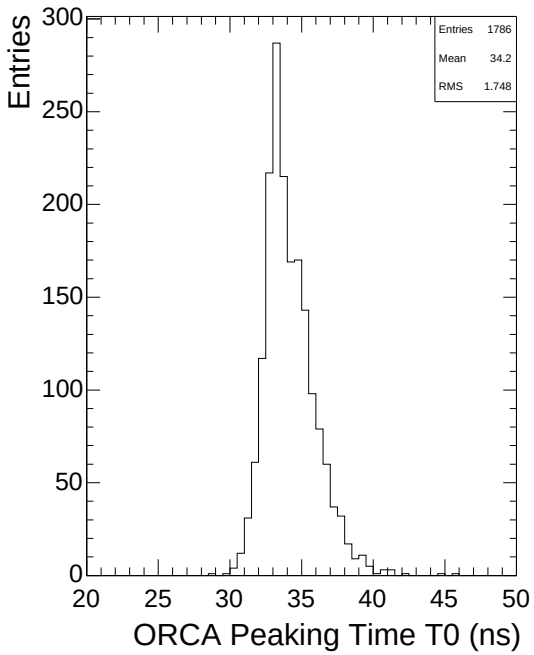

Figure 4: Distribution of the cathode strip peaking time, T_0, in ORCA.

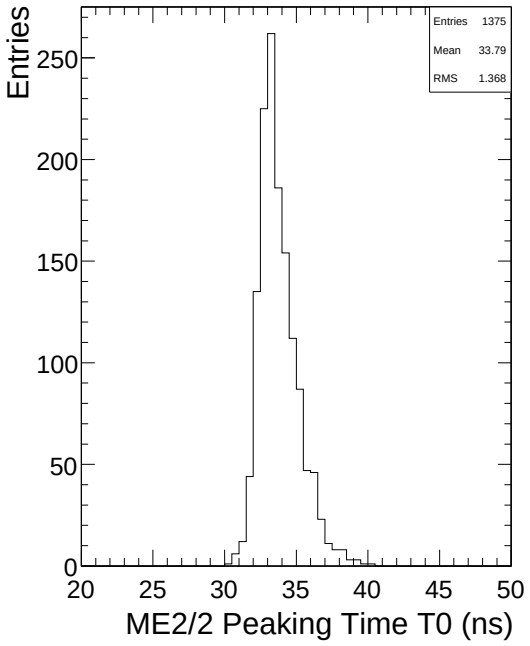

Figure 5: Distribution of the cathode strip peaking time, T_0, for pulses in an ME2/2 CSC from the test-beam data.

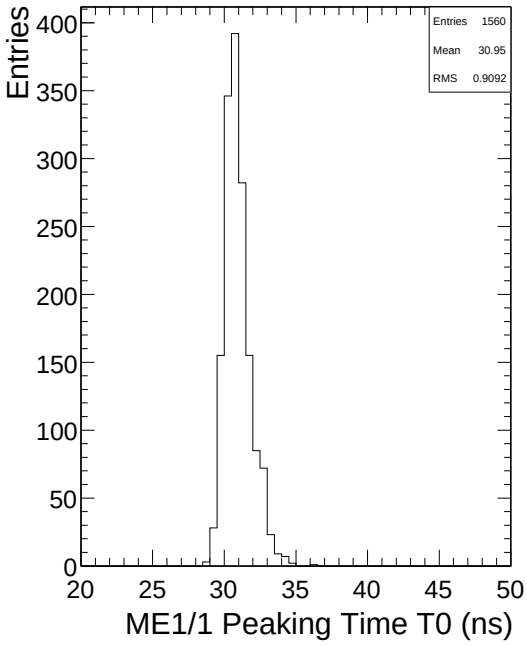

Figure 6: Similar to Figure 5 for a ME1/1 CSC from the test-beam data.

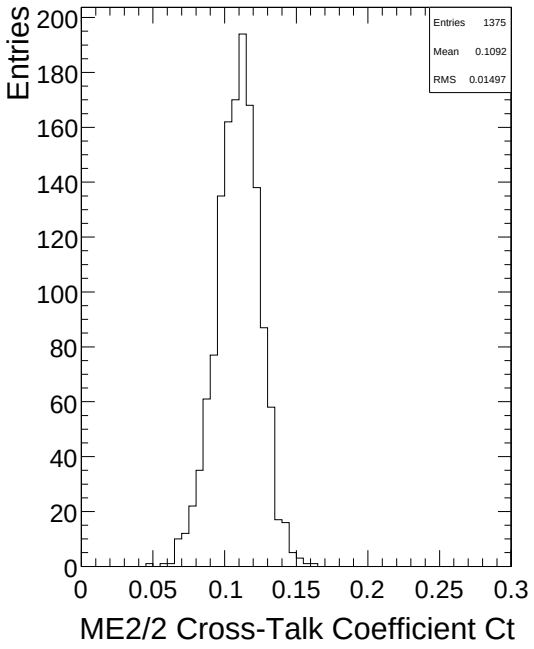

Figure 7: Distribution of the measured cross-talk coefficients in an ME2/2 CSC from test-beam data.

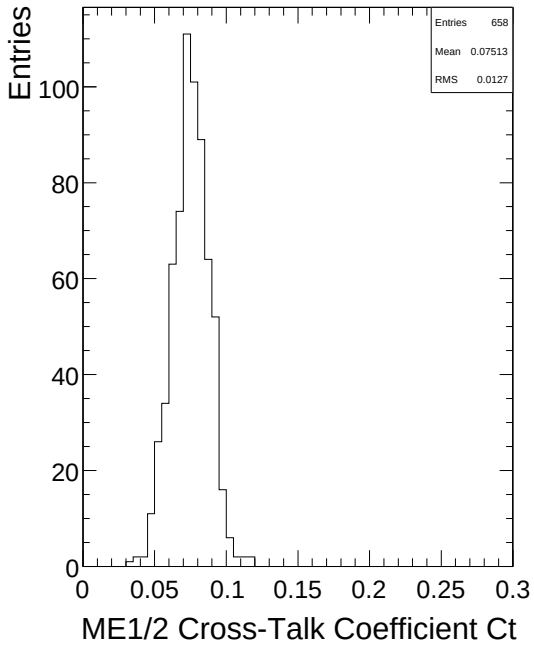

Figure 8: Similar to Figure 7 for a ME1/2 CSC from test-beam data.

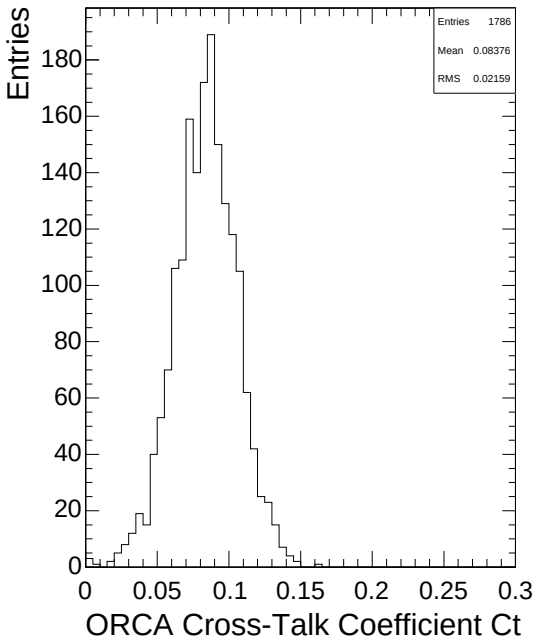

Figure 9: Distribution of the measured cross-talk coefficients in ME23/2 CSCs from the ORCA simulation.

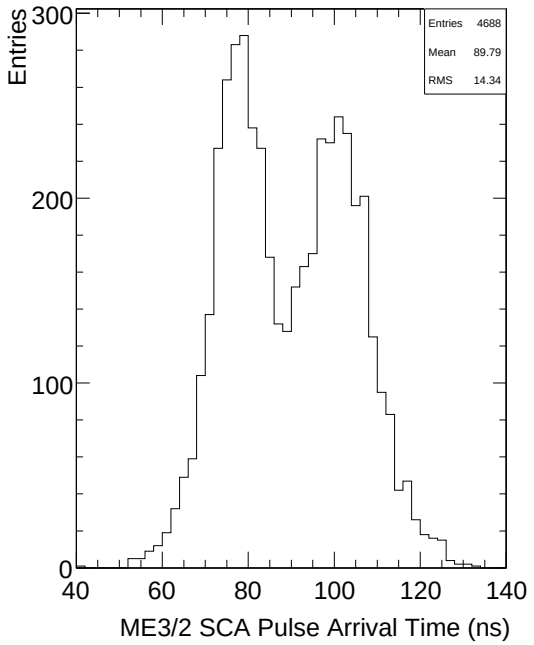

Figure 10: Distribution of the arrival time, T_s, for pulses in one layer of a ME3/2 CSC from test-beam data. The two peaks are due to the coupling of the 25 ns beam structure and the 50 ns SCA sampling time, as explained in the text.

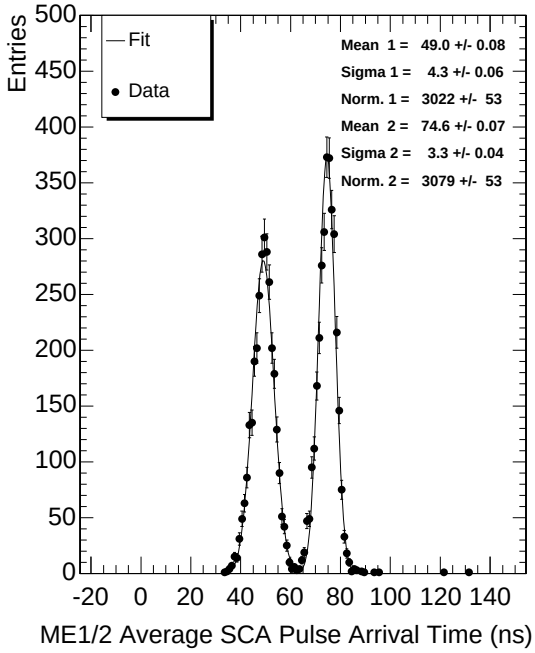

Figure 11: The muon beam-crossing time distribution in a ME1/2 CSC from test-beam data, along with the result of a fit to 2 Gaussians.

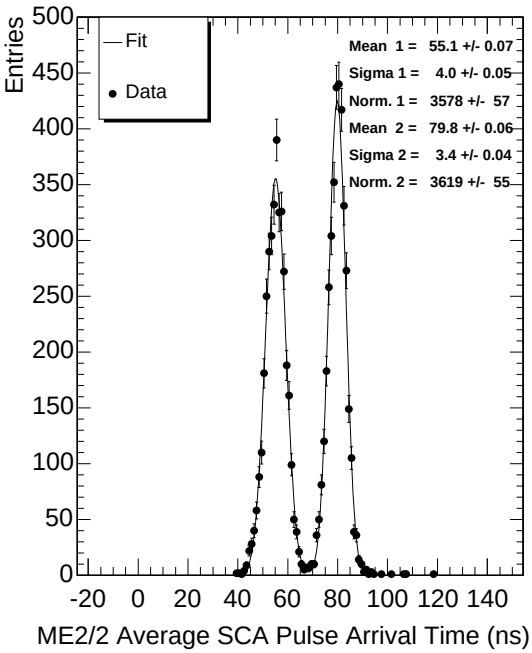

Figure 12: Similar to Figure 11 for a ME2/2 CSC from test-beam data.

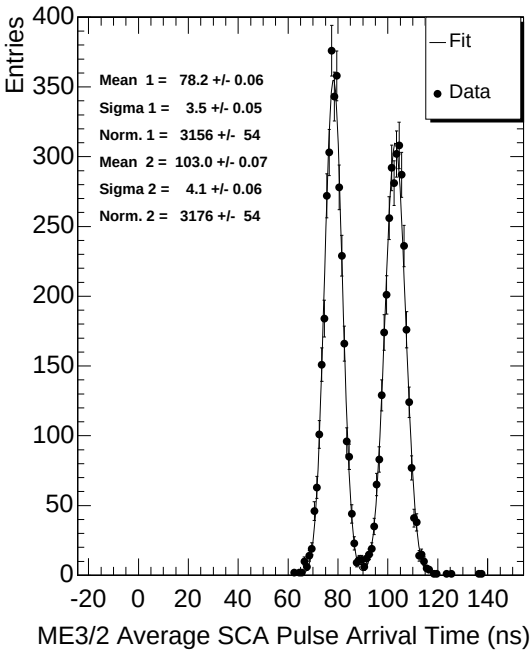

Figure 13: Similar to Figure 11 for a ME3/2 CSC from test-beam data.

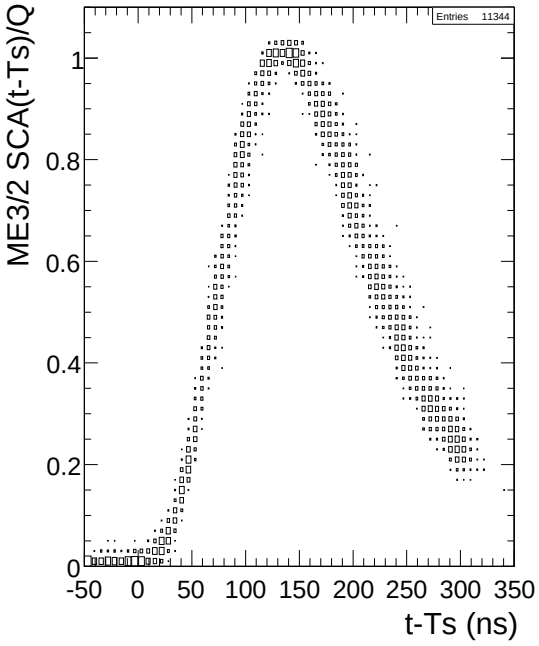

Figure 14: The cathode strip pulse shape in a ME3/2 CSC from test-beam data after subtraction of the pulse arrival time.

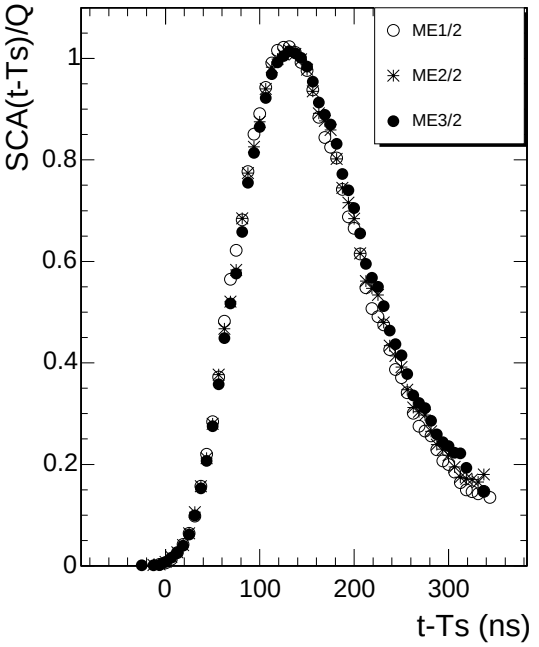

Figure 15: The average cathode strip pulse shape with subtracted T_s from test-beam data for ME1/2 (opened circles), ME2/2 (crosses), and ME3/2 (closed circles) CSCs.

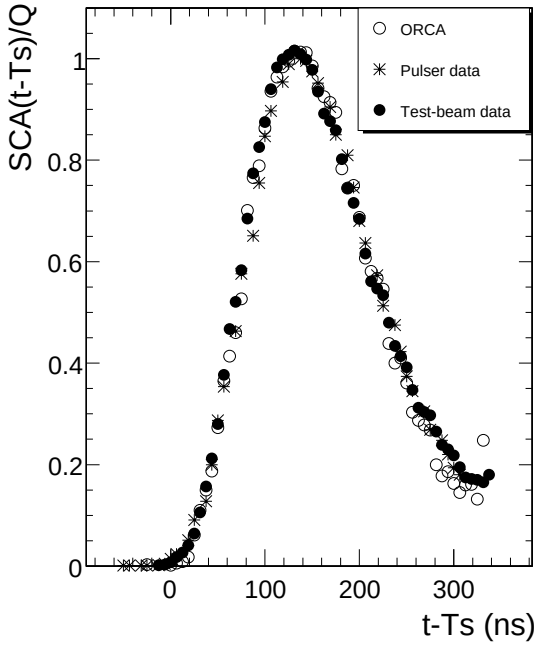

Figure 16: The average cathode strip pulse shape from the ORCA simulation (open circles), the pulser data (crosses), and the test beam (closed circles).

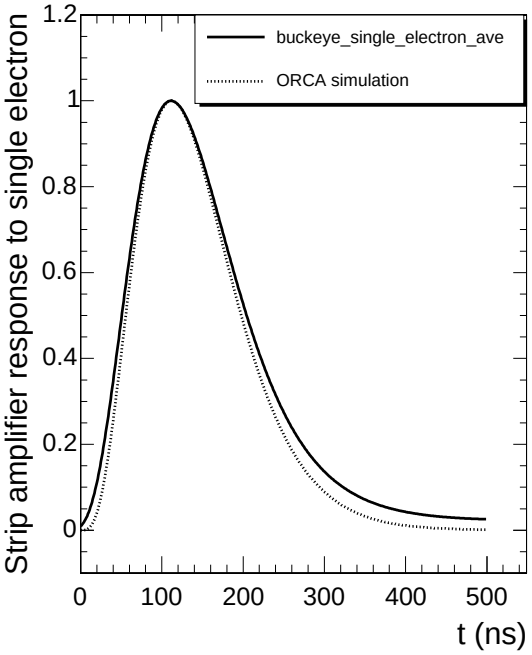

Figure 17: The cathode amplifier single-electron response function used in the ORCA simulation and a newer one from the production cathode front-end electronics.

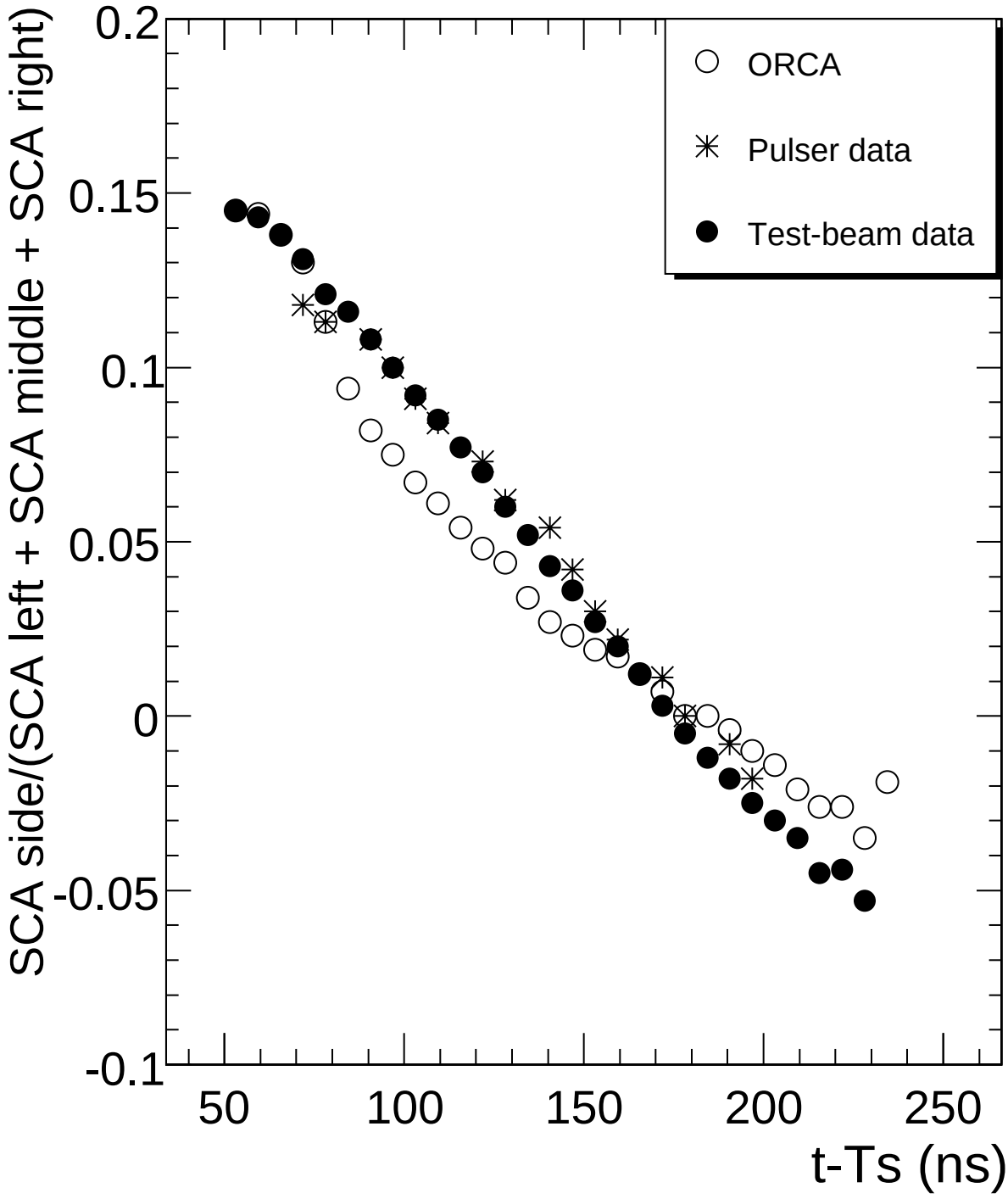

Figure 18: The measured average cross-talk ratios from the ORCA simulation (open circles), the pulser data (crosses), and the test beam (closed circles), as a function of time after the pulse arrival time, T_s.